CALIBRATION OF TIME–DOMAIN REFLECTOMETRY (TDR–315H) SENSOR FOR VOLUMETRIC WATER CONTENT MEASUREMENTS IN RECYCLED ROADBED MATERIALS

Van Nam Pham[1], Akihiro Matsuno[2], Ken Kawamoto[1]

[1]Saitama University, 255 Shimo–okubo, Sakura–ku, Saitama City, Saitama Prefecture 338–8570, Japan

[2]RISSHO University, 1700 Magechi, Kumagaya City, Saitama Prefecture, 360–0194, Japan

*Corresponding author: pvnam.nuce@gmail.com

(Received: May 03, 2025; Revised: June 19, 2025; Accepted: June 22, 2025)

DOI: 10.31130/ud-jst.2025.23(10C).662E

Abstract - Permeable pavement systems (PPS) are widely adopted in developed countries for urban flood control and heat island mitigation challenges, but have not yet been widely used in Vietnam. Monitoring volumetric water content (θ) in roadbed materials is essential for evaluating their performance for abovementioned challenges at pilot-scale. The Time Domain Reflectometry (TDR) technique is commonly used for measuring θ but requires a material–specific calibration for θ values. This study aims to establish calibration curves for roadbed materials by using a commercially available sensor of TDR-315H. Two types of materials were tested in the laboratory: (i) unbound roadbase materials including recycled concrete aggregates (RCA), RCA blended with autoclaved aerated concrete grains, and natural aggregates, and (ii) RCA combined with recycled brick aggregates and cement as a bound porous surface. The results showed that sensor manufacturing variability was negligible, and specific calibration curves were successfully developed for each material.

Key words - Time domain reflectometry; calibration curve; volumetric water content; roadbed materials

1. Introduction

Permeable pavement systems (PPS) have been recognized as sustainable drainage systems that contribute to addressing various challenges in urban areas, such as controlling urban floods, improving groundwater quality, and mitigating the urban heat island (UHI) in many developed countries. However, a review work on challenges to the adoption of PPS in Vietnam [1] revealed that PPS has not yet been widely used in Vietnam, and one of the challenges is that policymakers have not yet recognized PPS practice as being beneficial under the conditions of Vietnam. To evidence the benefits PPS can bring under the conditions of Vietnam, establishing a pilot–scale monitoring system to monitor required parameters/properties for evaluating the effectiveness of PPS in controlling urban flooding and mitigating the UHI becomes important. The volumetric water content (θ) of roadbed material stands out as one of the most important properties required to evaluate the above challenges.

Time Domain Reflectometry (TDR) is a widely used electromagnetic technique for determining the volumetric water content (θ) of soil. Since Topp et al. [2] introduced a general calibration equation linking TDR–measured dielectric constant (ε) to θ, numerous alternative calibration models have been developed by various researchers (e.g., [3–4]). Previous studies have shown that the dielectric constant is affected by factors such as water content and density [5], bound water [6], temperature [7], bulk electrical conductivity [8], and soil salt content [9].

Estimating volumetric water content using a TDR sensor often requires a soil–specific calibration between the ε and θ in the laboratory [10]. The TDR–315H sensor (Acclima Inc., USA), recently commercialized by Acclima Inc., USA, is designed to measure θ in soils [11]. Compared to other sensors in the TDR–315 series, the TDR–315H features several improvements, including a faster rise time, shaped incident wave, lower power consumption, and very fast response time [12]. Although full waveforms can be acquired from TDR–315 series sensors (including the TDR–315H) via a specialized interface, the sensor is primarily designed to output processed data which is automatically converted to dielectric constant via a comparative interface (e.g., PC400, Campbell Scientific, Inc., USA) [13]. Owing to these benefits, some studies have used this sensor to estimate soil θ in practice (e.g., [11, 14]) without calibration (i.e., relying on default models or manufacturer–provided calibration curves). However, this assumption may not hold for fundamentally different coarse materials, such as roadbed materials. Till now, there have been limited studies on calibration curves (ε vs. θ) using the TDR–315H for roadbed materials. Therefore, this study aims to: (i) evaluate manufacturing variability by measuring the dielectric constants of well–known reference materials (distilled water and air), and (ii) establish calibration curves for the TDR–315H for roadbed materials.

2. Materials and methods

2.1. Materials

For the unbound base materials, recycled concrete aggregates (RCA) were produced from waste concrete collected at a construction and demolition waste dumping site in Hanoi, Vietnam. Scrap autoclaved aerated concrete (AAC) obtained from Viglacera Corp. in Bac Ninh Province, Vietnam, was crushed using a stainless–steel hammer, while RCA was crushed using a jaw and hammer crusher. Two RCA–AAC blends were prepared based on mass substitution rates (*f*): 0% (RCA100%) and 30% (RCA70% + AAC30%). Additionally, a natural aggregate sample (NA100%) was included for comparison.

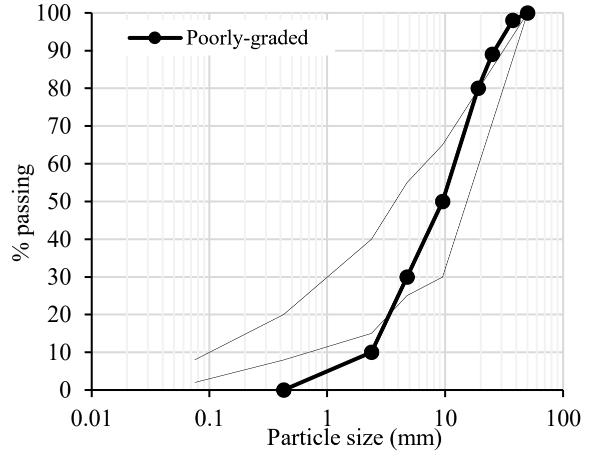

***Figure 1.** Particle size distributions of the tested materials (solid line) in this study. The boundaries (dashed lines) for subbase materials prescribed in TCVN 8857:2011 [19] were given*

All materials were classified as poorly graded according to ASTM D2487:2006 [15], and their particle size distributions are shown in Figure 1. While some fractions fell outside the recommended boundaries in Figure 1, all samples were confirmed to meet roadbed bearing capacity requirements [16]. The 30% AAC substitution rate was selected due to its optimal balance of water retention and structural integrity [16–17]. The initial water contents for compaction were 2%, 10.7%, and 24.5% for NA100%, RCA100%, and RCA70%+AAC30%, respectively. The initial water content refers to the water content during the compaction. TDR–315H sensors were vertically installed at the center of a Modified Proctor compaction mold (inner diameter: 15 cm; height: 12.5 cm) that was sufficiently large to allow smooth compaction and prevent sensor damage. The materials were then compacted to achieve dry densities of 1.97, 1.70, and 1.30 g/cm^3, respectively, which approximates the maximum dry densities obtained by the Modified Proctor method [18].

For the bound porous pavement surface, RCA and recycled brick aggregates (2.5–5 mm) were mixed with cement and water at a water–cement ratio of 0.25 (i.e., 95/380) to produce the porous surface layer. A water–reducing agent was added during mixing. The proportions of aggregates, water, and cement used in the concrete mix design are detailed in Table 1. Two transparent, rigid plastic cylindrical molds, which are identical in dimensions to the Modified Proctor compaction mold, were joined together using glue. A TDR–315H was vertically placed in the center of the mold, and the samples were compacted by hand using a pestle. Duplicate specimens, labelled K–Ground 1 and K–Ground 2, were prepared with technical support from ECOSYSTEM Inc., Japan [20–21]. The resulting dry densities after compaction were 1.66 g/cm^3 and 1.39 g/cm^3, respectively. The basic physical properties of the tested samples are summarized in Table 2.

***Table 1.** The comparison of clustering result*

Components	W	C	RCA	RCB	Water–reducing agent
Amount (kg)	95	380	658	745	3.8

W: Water, C: Cement, RCB: Recycled clay brick

***Table 2.** Basic physical properties of the tested samples used in this study*

Sample	Surface layer		Roadbase layer		
	K–Ground 1	K– Ground 2	NA100%	RCA100%	RCA70%+AAC30%
Sensor	TDR 1–1	TDR 1–2	TDR 2–1	TDR 2–3	TDR 2–5
r_s	2.69	2.69	2.98	2.68	2.65
g (g/cm^3)	1.66	1.39	1.97	1.70	1.30
Φ	0.38	0.48	0.27	0.33	0.45

r_s: specific density, g: Dry density, Φ: total porosity

2.2. Sensor description

The TDR–315H is a high-precision time domain reflectometry (TDR) sensor designed for soil moisture and geophysical measurements. It supports the industry-standard SDI–12 communication protocol and is compatible with any data logger equipped with an SDI–12–compliant port, making it highly adaptable for various field applications [22]. The sensor features a planar three-conductor transmission line, 150 mm in length (see Figure 2), composed of a central rod for transmitting the incident pulse and two outer rods serving as grounds. Each rod has a diameter of 3.5 mm, with a spacing of 19 mm between them, forming a defined electromagnetic field for accurate measurements. Internally, all TDR–315H sensors use a standardized printed circuit board assembly. This includes a step function generator, a precision time base generator, a 5-ps resolution waveform digitizer, a thermistor for temperature compensation, and communication circuitry-all encapsulated within the sensor head for durability and protection. The step function generator produces an 80 MHz step pulse with a 20–80% rise time of 64 ps. The TDR circuitry is directly coupled to the electrodes to ensure high-fidelity signal transmission and reflection analysis [22].

A summary of the sensor’s key measurable parameters, including electrical characteristics and structural dimensions, is provided in Table 3.

***Table 3.** Key measurable measurements of the TDR–315H sensor*

Parameters	Φ	Dielectric constant (ε)	BEC	T
Unit	%		μS/cm	ºC
Range	0 ~100	1 ~ 80	0 ~ 5000	– 40 ~ 60

θ: Volumetric water content, BEC: Bulk electrical conductivity, T: Medium temperature

2.3. Measurements of volumetric water content and dielectric constant using TDR–315H sensor

For the measurements of the ε and θ of roadbed materials, a typical schematic of the TDR sensor setup for K–Ground samples is shown in Figure 2. The TDR sensor was connected to a data logger (CR1000X, Campbell Scientific, Logan, UT, USA) and a laptop. The PC400 interface software (Campbell Scientific) was used to record the dielectric constant. Measurements began at the initial water content. Following this, the samples were fully saturated for one week and then gradually de–saturated by gravimetric water loss.

The drying process was conducted at room temperature (18~25°C). For the bound porous surface samples (i.e., K–Ground 1 and 2), free water was monitored visually several times until no visible water remained (approximately within the first 10 minutes)

For the unbound roadbase samples (i.e., RCA100%, RCA70%+AAC30%, and NA100%), due to their high capillary water content, few samples at intermediate moisture ranges were measured for volumetric water content and dielectric constant. Although achieving completely uniform water content throughout the samples, especially in the vertical direction, is unrealistic, the sensor rod was placed horizontally during measurements to ensure consistent water content across all sensor contact points.

Figure 2. *Typical schematic of the TDR–315H sensor setup*

The volumetric water content at each stage was determined based on the weight of water lost during the controlled de-saturation process. Following this, the samples were oven-dried at a constant temperature of 30 °C for a period of two weeks. This relatively low drying temperature was intentionally selected to prevent potential damage to the TDR sensors embedded in the samples. After drying, the samples were transferred to a climate-controlled room and stored under stable environmental conditions, specifically, at 20 °C and 60% relative humidity for an additional two weeks to ensure equilibrium moisture conditions before further testing. At each stage corresponding to a specific water content level, the dielectric constant of the material was measured and recorded using the TDR sensors. For reference and calibration purposes, additional TDR measurements were conducted using distilled water and air as standard media. The procedure for these measurements followed the same methodology as that applied to the roadbed material samples, ensuring consistency in the experimental approach.

3. Result analysis

3.1. Dielectric constant of distilled water and air

The observed dielectric constant of distilled water and air was tabulated in Table 4. The temperature of distilled water (T_{water}) was in the range of 18~19.5 °C, while that for air (T_{air}) was 19~21°C. There was slightly a slight difference in temperature between each measurement for distilled water (i.e., TDR 1–1 and 1–2 were performed under T_{water} of 18°C, while that for TDR 2–1 and 2–2 and 2–3 was 19.5°C), and for air (i.e., TDR 1–1 and 1–2 were performed under T_{air} of 19°C, while that for TDR 2–1 and 2–2, and 2–3 was 21°C). Despite this, the observed dielectric constants remained stable, ranging from 78 to 80 for water and around 1.0 for air. The average values of 79 (water) and 1.0 (air) closely match well–known reference values (e.g., [23]), indicating that manufacturing variations among the TDR sensors were negligible. Moreover, slight changes in medium temperature did not significantly affect the dielectric constant measurements.

Table 4. *Key measurable measurements of the TDR–315H sensor*

Sensor	Air		Distilled water	
	T_{air} (°C)	ε	T_{water} (°C)	ε
TDR 1–1	19.0	1.1	18.0	80
TDR 1–2	19.0	1.0	18.0	78
TDR 2–1	21.0	1.0	19.5	79
TDR 2–3	21.0	1.0	19.5	79
TDR 2–5	21.0	1.0	19.5	79

T_{air}, T_{water}: Temperature of air and distilled water at the time of measurements determined by thermometer

3.2. Calibration curves for TDR–315H sensor in roadbed materials

The observed dielectric constant of porous pavement surface materials (K–Ground 1 and 2) and roadbase materials (NA100%, RCA100%, and RCA70% + AAC30%) is shown in Figures 3a and 3b. In Figure 3b, the reference materials from the literature were given. The well–known empirical dielectric constant and soil water content (ε vs. θ) relationship developed by Topp et al. [2] has been plotted as follows:

$$\varepsilon = 3.03 + 9.3\theta + 146\theta^2 - 76.7\theta^3 \quad (1)$$

In this study, because the roadbed materials exhibited a wide range of dry bulk densities, the semi–physical equation proposed by Malicki et al. [3], which takes the dry bulk density (γ) into account, was adopted to define the lower and upper boundaries of the calibration range. The equation by Malicki et al. [3] is expressed as:

$$\theta = \varepsilon^{0.5} - 0.819 - 0.168g - 0.159g^2)/(7.17 + 1.18g) \quad (2)$$

where g is the dry bulk density (g/cm^3). In this study, the lower dry bulk density was assumed to be 0.7 g/cm³, as observed in the case of AAC100% [16], while the upper bound was set to 2.98 g/cm³ (Table 2), corresponding to the theoretical specific gravity of the NA100% used.

Looking at Figure 3a, the calibration curve (ε vs. θ) for K–Ground 1 and 2 showed two distinct trends. A single polynomial curve, commonly used for soil or sand calibration (e.g., Figure 3b), was not applicable to these samples. It is noted that during the experiment, the measurement of dielectric constant and the corresponding θ at the turning point was performed by de–saturating the gravitational (free) water by gravity. Therefore, it is assumed that the turning point represents the transition between gravitational water and capillary water states. It is observed that from full saturation to the point just before the gravitational water was depleted, the dielectric constant of the TDR sensor was highly sensitive to changes in θ. In contrast, in the range from just after gravitational water depletion to the air–dried condition (i.e., dominated by hygroscopic or bound water), the dielectric response to θ was less pronounced. The decrease in θ before the gravitational water state ends probably leads to the existence of air surrounding the TDR sensor and a significant decrease in ε value with a small decrease in θ. Once the gravitational water had drained, only bound water remained, and the surrounding air had a dominant influence, resulting in reduced ε variability with further changes in θ. This is expected, as the dielectric constant of free water is significantly higher than that of bound water [6]. The observed calibration (ε vs. θ) values for K–Ground 1 and 2 (as well as for the roadbed materials shown in Figure 3b) fell within the upper and lower boundaries using Malicki et al. [3] proposed model, which incorporates the effect of dry bulk density.

Looking at Figure 3b, the calibration curves for NA100%, RCA100%, and RCA70%+AAC30%, in contrast to K–Ground 1 and 2 samples, showed smoother curves and could be well fitted using polynomial equations.

Notably, for the same θ, the ε differed significantly across materials, particularly between NA100% and the other two RCA–based mixtures. This is probably due to the difference in materials used and geometry. The results from water retention curves (e.g., [17]) and pore size density (e.g., [24–25]) for these materials indicate that NA100% exhibited a sigmoidal curve, while that for RCA100% and RCA70%+AAC30% were bimodal curves.

The pore size distribution of NA100% is assumed to be mainly contributed by the macro pore water (e.g., free pore water) formed between the particles, while that for RCA100% and RCA70%+AAC30% was micropores formed by between particles and/or particles itself.

The references of fine particle materials such as silty loam [9], sand and calcined clay [26], using the same TDR sensors, exhibited slight differences; however, overall, they are much less sensitive than coarse materials (roadbed materials) in this study. This indicates the importance of calibration of TDR sensors, especially for coarse materials. The widely used calibration curve proposed by Topp et al. [2] captured the general trend reasonably well for soils, sands, and RCA–AAC materials, especially under low water content conditions (Figure 3b). Material–specific calibration curves for all tested roadbed materials are presented in Figures 3a and 3b.

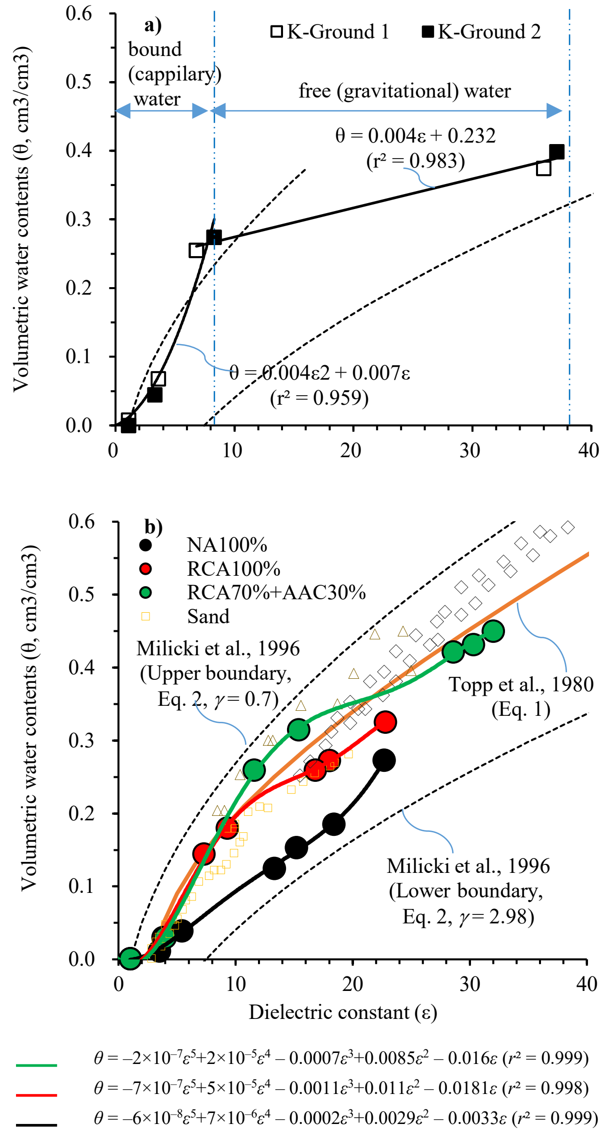

Figure 3. *Calibration curves of the tested materials used in this study: (a) bound porous surface material and (b) unbound roadbed materials. Reference calibration data using the same TDR–315H from previous studies [9, 26] was given*

Nevertheless, the observed differences in calibration curves across varying dry densities for roadbed materials strongly indicate that dry density is a critical factor influencing TDR–based calibration. Therefore, the development of calibration models for roadbed materials, particularly those incorporating RCA, AAC, and NA should explicitly account for dry density to improve measurement accuracy.

4. Conclusion

A series of laboratory tests were carried out to measure the volumetric water content and corresponding dielectric constant using TDR–315H for various recycled roadbed materials made from construction waste materials.

The results showed that manufacturing variations among the TDR–315H used in this study were negligible. Additionally, the measured dielectric constants for distilled water and air remained stable, even with temperature variations of a few degrees Celsius.

The calibration curves developed for different materials demonstrated that accurate estimation of volumetric water content using TDR–315H is material–specific, particularly for coarse–grained materials such as those used in roadbeds. Therefore, material–specific calibration is essential prior to practical application. The established calibration curves for NA, RCA, RCA mixed with AAC, and RCA mixed with recycled brick and cement can be used as practical references for estimating θ in these roadbed materials. In cases where arbitrary proportions of AAC are mixed with RCA and specific calibration curves are unavailable, models that incorporate dry density such as that proposed by Malicki et al. [3], can be considered as a reasonable alternative.

Acknowledgments: This research was supported by the project of Japan Science and Technology Agency (JST) – Japan International Cooperation Agency (JICA) on Science and Technology Research Partnership for Sustainable Development (SATREPS) (No. JPMJSA1701) and the research grant from Research Bureau of Saitama University. We thanks to ECOSYSTEM Inc., Japan and Hanoi Univeristy of Civil Engineering for supporting the sample preparation of K-Ground.

REFERENCES

[1] P.V. Nam, K. Kawamoto, N.T. Dung, T.T. Kien, and N. H. Giang, "Review of Water and Heat Balances and Challenges To Adoption of Permeable Pavement System in Vietnam," *Int. J. GEOMATE,* vol. 24, no. 103, pp. 84–95, 2023. https://doi: 10.21660/2023.103.g12169.

[2] G. C. Topp, J. L. Davis, and A. P. Annan, "Electromagnetic determination of soil water content: Measurements in coaxial transmission lines," *Water Resour. Res*., vol. 16, no. 3, pp. 574–582, 1980. https://doi: 10.1029/WR016i003p00574.

[3] M. A. Malicki, R. Plagge, and C. H. Roth, "Improving the calibration of dielectric TDR soil moisture determination taking into account the solid soil," *Eur. J. Soil Sci*., vol. 47, no. 3, pp. 357–366, 1996. https://doi: 10.1111/j.1365–2389.1996.tb01409.x.

[4] T. Miyamoto, R. Kobayashi, T. Annaka, and J. Chikushi, "Applicability of multiple length TDR probes to measure water distributions in an Andisol under different tillage systems in Japan," *Soil Tillage Res*., vol. 60, no. 1–2, pp. 91–99, 2001. https://doi: 10.1016/S0167–1987(01)00172–6.

[5] L. M. Thring, D. Boddice, N. Metje, G. Curioni, D. N. Chapman, and L. Pring, "Factors affecting soil permittivity and proposals to obtain gravimetric water content from time domain reflectometry measurements," *Can. Geotech. J*., vol. 51, no. 11, pp. 1303–1317, 2014. https://doi: 10.1139/cgj–2013–0313.

[6] D. A. Boyarskii, V. V. Tikhonov, and N. Y. Komarova, "Model of dielectric constant of bound water in soil for applications of microwave remote sensing," *J. Electromagn. Waves Appl*., vol. 16, no. 3, pp. 411–412, 2002. https://doi: 10.1163/156939302X01227.

[7] S. Wojciech, "Time Domain Reflectometry: Temperature–dependent Measurements of Soil Dielectric Permittivity," Electromagn. Waves, 2011.

[8] M. Bittelli, F. Salvatorelli, and P. R. Pisa, "Correction of TDR–based soil water content measurements in conductive soils," *Geoderma*, vol. 143, no. 1–2, pp. 133–142, 2008. https://doi: 10.1016/j.geoderma.2007.10.022.

[9] Q. Qi, H. Yang, Q. Zhou, X. Han, Z. Jia, Y. Jiang, Z. Chen, L. Hou, and S. Mei "Performance of Soil Moisture Sensors at Different Salinity Levels: Comparative Analysis and Calibration," *Sensors*, vol. 24, no. 19, pp. 1–16, 2024. https://doi.org/10.3390/s24196323

[10] H. Quinones, P. Ruelle, and I. Nemeth, "Comparison of three calibration procedures for tdr soil moisture sensors," *Irrig. Drain.*, vol. 52, no. 3, pp. 203–217, 2003. https://doi: 10.1002/ird.95.

[11] G. W. Marek, S. Evett, T. H. Marek, D. O. Porter, and R. C. Schwartz, "Field Evaluation of Conventional and Downhole Tdr Soil Water Sensors for Irrigation Scheduling in a Clay Loam Soil," *Appl. Eng. Agric*., vol. 39, no. 5, pp. 495–507, 2023. https://doi: 10.13031/aea.15574.

[12] Data Sheet True TDR–315H soil water temperature, Acclima, Inc. USA, 2019.

[13] R. C. Schwartz, S. R. Evett, S. K. Anderson, and D. J. Anderson, "Evaluation of a Direct–Coupled Time–Domain Reflectometry for Determination of Soil Water Content and Bulk Electrical Conductivity," *Vadose Zo. J*., vol. 15, no. 1, pp. 1–8, 2016. https://doi: 10.2136/vzj2015.08.0115.

[14] Y. Wang, Z. Zhang, Z. Guo, Y. Chen, J. Yang, and X. Peng, "In–situ measuring and predicting dynamics of soil bulk density in a non–rigid soil as affected by tillage practices: Effects of soil subsidence and shrinkage," *Soil Tillage Res*., vol. 234, p. 105818, 2023. https://doi: 10.1016/j.still.2023.105818.

[15] Standard Practice for Classification of Soils for Engineering Purposes (Unified Soil Classification System), American Society for Testing and Materials (ASTM), West Conshohocken PA, 2006.

[16] P. V. Nam, N. T. Dung, N. H. Giang, and K. Kawamoto, "Mechanical, hydraulic, and particle breakage properties of recycled concrete aggregates blended with autoclaved aerated concrete (AAC) grains for unbound road base and subbase materials in Vietnam," *J. Mater. Cycles Waste Manag*., vol. 26, no. 2, pp. 845–859, 2024. https://doi.org/10.1007/s10163–023–01858–7.

[17] P. V. Nam, N. T. Dung, N. H. Giang, and K. Kawamoto, "Unsaturated hydraulic properties of recycled concrete aggregates blended with autoclaved aerated concrete grains for unbound road base materials in Vietnam," *J. Mater. Cycles Waste Manag*., no. 0123456789, 2024. https://doi: 10.1007/s10163–024–02134–y.

[18] Standard Test Methods for Laboratory Compaction Characteristics of Soil Using Modified Effort (56,000 ft–lbf/ft3 (2,700 kN–m/m3)), American Society for Testing and Materials (ASTM), ASTM International, West Conshohocken, PA, 2012.

[19] *Natural Aggregate for Road Pavement Layers – Specification for Material,* Construction and Acceptance, TCVN 8857:2011.

[20] ECO SYSTEM Inc., "K-Ground C Permeable Paving Material with Aggregate Made from Recycled Roof Tiles", *eco-system.ne.jp*. [Online]. Available: https://eco-system.ne.jp/bus_info_eng.html [Accessed October 22, 2025].

[21] N. K. Tuan, K. Kawamoto, M. Suzuki, Y. Tanaka, P. Q. Minh, N. H. Giang, and N. T. Dung, "Evaluating the thermal performance of permeable pavements: A case study in an urban Area of Vietnam," *Global Environmental Research*, vol. 28, no. 1, pp. 45–52, 2024. https://doi: 10.57466/ger.28.1_45.

[22] Acclima TDR Sensor User Manual For Sensor Models: TDR305H, TDR310H, TDR315H, Acclima, Inc. USA.

[23] J. M. Schneider and D. Fratta, "Time–domain reflectometry – parametric study for the evaluation of physical properties in soils," *Can. Geotech. J*., vol. 46, no. 7, pp. 753–767, 2009. https://doi: 10.1139/T09–018.

[24] P.V. Nam, N. Q. Cuong, N. H. Giang, and K. Kawamoto, "Unsaturated hydraulic property of recycled concrete aggregates blended with autoclaved aerated concrete grains for unbound road base and subbase materials in Vietnam," *IOP Conf. Ser. Mater. Sci. Eng*., vol. 1289, no. 1, p. 012100, 2023. https://doi: 10.1088/1757–899X/1289/1/012100.

[25] T. H. Nam, K. Kawamoto, N. H. Giang, T. Komatsu, and P. Moldrup, "Diffusive and convective transport properties and pore–network characteristics of recycled, compacted concrete aggregates for use as road pavement materials," *Constr. Build. Mater*., vol. 457, 2024. https:// doi: 10.1016/j.conbuildmat.2024.139460.

[26] C. Y. Chang, "*Electromagnetic Sensor Sampling Volumes and Water Content Calibration in Coarse–Textured Porous Media Using Layered Mixing Theories*," Master's thesis, Utah State Univ, United States, 2025.